Effect of Ionic Charge on the CH···π Hydrogen Bond

ARTICLE *in* THE JOURNAL OF PHYSICAL CHEMISTRY A · SEPTEMBER 2014

Impact Factor: 2.69 · DOI: 10.1021/jp5070598 · Source: PubMed

2 AUTHORS:

Binod Nepal
Utah State University
10 PUBLICATIONS **37** CITATIONS
SEE PROFILE

Steve Scheiner
Utah State University
366 PUBLICATIONS **11,212** CITATIONS
SEE PROFILE

THE JOURNAL OF PHYSICAL CHEMISTRY A

Article

pubs.acs.org/JPCA

Effect of Ionic Charge on the CH···π Hydrogen Bond

Binod Nepal and Steve Scheiner*

Department of Chemistry and Biochemistry, Utah State University, Logan, Utah 84322-0300, United States

Supporting Information

ABSTRACT: The CH···π hydrogen bonds (HBs) between trimethylamine (TMA) and an assortment of π-systems are generally weaker than those in which CF_3H serves as a proton donor, despite the larger number of CH groups available to serve as donors in the amine. The added positive charge of tetramethylammonium (TMA+) enhances the binding energy by a factor between 4 and 7. The strongest such interaction for TMA+ occurs with indole, bound by 15.5 kcal/mol. Changing from ionic CH···π to NH···π further strengthens the interaction. Conjugation of the π-system improves its proton-accepting capacity, which is further enhanced by aromaticity. Dispersion plays a major role in CH···π HBs: It is the prime contributor in the neutral HBs of TMA, and comparable to Coulombic forces for CF_3H and even in ionic CH···π HBs of TMA+. Many of the results can be understood on the basis of a combination of electrostatic potentials and charge transfers.

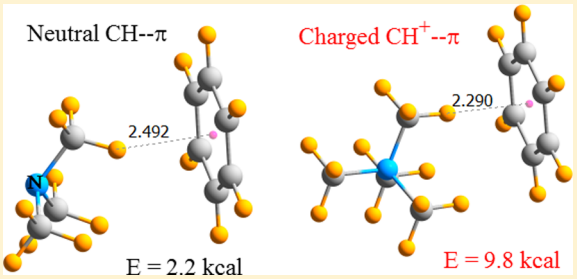

INTRODUCTION

Among an assortment of noncovalent interactions that have been recognized over the years,[1,2] hydrogen bonds (HBs) are generally considered the most widespread and important.[3,4] The original consideration of N, O, and F as HB donor and acceptor atoms in a DH···A arrangement has been expanded over the years to include other less electronegative atoms like S, Cl, and C.[5−10] Of these, the ability of CH to serve as a proton donor has been perhaps most extensively scrutinized, and this growing recognition of CH···O HBs has spawned a diverse literature database that has informed a wide swath of chemistry and biochemistry.[11−18]

In addition to lone pairs, the source of electrons may reside instead in the π-electron system of the proton-acceptor group. Although generally weak, the CH···π HB makes its presence felt in a large number of instances.[19−23] As one example, Brandl et al.[24] studied a set of more than 1000 different protein structures which were found to contain over 30 000 C−H π interactions which contribute significantly to the overall stability of the proteins.

Under most circumstances, CH···π HBs are weaker than their classical analogues. For example, the binding energy of methane with the benzene ring, primarily attributed to dispersion, is only around 1.4 kcal/mol.[25,26] On the other hand, in other types of HBs, the introduction of a positive charge into the proton donor, or negative on the acceptor, can very substantially enhance the interaction.[27−31] For example, calculations[32] found a complex between trimethylammonium ion and the O acceptor atom of methyl acetate that relied solely on CH^+···O HBs was bound by 13 kcal/mol. More recently, this research group showed[33] that the introduction of a positive charge on the proton donor substantially enhanced the binding energy of several CH···O HBs, by a factor of 4−9. It is tempting to presume that a similar charge-induced magnification might be operating in CH···π HBs as well. Indeed, Dougherty's group synthesized a large number of host molecules[34] which can extract cations from aqueous solution employing ionic CH···π and NH···π HBs. However, there has been little detailed scrutiny of this issue, so a quantitative assessment of the potential strength of CH···π HBs is lacking and perhaps overdue.

Information about this topic ought to have implications for biological systems, including stability of proteins,[35] biochemical reactions,[36] controlling stereochemistry in organic synthesis,[37] and molecular crystal structure.[38] For example, there is a preference within proteins for cationic amine side chain groups as in lysine and arginine to be oriented[39] toward a nearby aromatic side chain so as to engage in NH^+···π HBs with them. However, the charge exerts its effect further along the chain, as in lysine−tryptophan interaction, where the CH_2 group adjacent to the NH_3^+ participates in a CH···π interaction. In another example, D-dopamine binds to the D-2 receptor site[36] via CH···π HBs involving the methylene protons β to the NH_3^+.

Even though a good deal of experimental data reinforce the important role played by ionic CH···π and NH···π bonds in a variety of natural phenomena and chemical reactions, there remain a number of unanswered questions. What factors influence the strength of these bonds, and what is the limit on such strength? How does a single π-bond as in ethylene compare with a series of conjugated π-bonds or an aromatic system? Is a single CH···π HB preferable to bifurcated or trifurcated arrangements? From a fundamental perspective, is the CH···π pairing a true HB or is it merely a simple

Received: July 15, 2014
Revised: August 28, 2014
Published: September 7, 2014

dx.doi.org/10.1021/jp5070598 | J. Phys. Chem. A 2014, 118, 9575−9587

Table 1. Binding Energies (kcal/mol) of CH···π and NH···π Complexes after Counterpoise Correction and Angular Distortion of CH···π HBs for F_3CH as a Proton Donor

proton acceptor	F_3CH	θ(CH···c[a]) (deg)	$N(CH_3)_3$	$N(CH_3)_4^+$	NH_4^+
ethylene	1.60	172.7	0.83	4.69	11.05
acetylene	1.57	177.8	0.71	4.64	10.50
butadiene	2.53		1.66	7.12	14.58
benzene	3.72	179.0	2.17	9.75	18.68
phenol	3.88	147.8	2.69	11.42	19.15
imidazole	4.08	133.9	4.45	11.33[d]	15.68[d]
indole	4.34,[b] 4.87[c]	144.5,[b] 149.4[c]	3.79	15.51	25.04

[a]c represents center of bond or ring. [b]CH poised above 5-membered ring. [c]CH poised above 6-membered ring. [d]Optimized with N of the proton donor restricted to the imidazole perpendicular.

Coulombic interaction? Precisely how does charge affect the nature and strength of each interaction, and what are the effects on the preferred geometry?

Quantum mechanical techniques offer an essential means of addressing these questions. In this work, a variety of both CH and NH proton donors are considered for purposes of comparison. CF_3H is a small and relatively simple molecule whose three F atoms impart a fairly strong polar character to the CH bond, making it a potent proton donor. The CH bonds in $N(CH_3)_3$ are less polar, but their number might make up for the weakness of any one individual CH···π bond. This molecule also facilitates a detailed comparison of single vs bifurcated and even trifurcated HBs. The effects of adding a charge can then be easily isolated and studied by consideration of the very similar $N(CH_3)_4^+$ ion. Comparison with the NH donor groups of NH_4^+ reveals any intrinsic differences between NH and CH HBs.

In terms of proton acceptors, a variety of π systems were considered. Ethylene and acetylene both contain a single C—C connection, whereas 1,3-butadiene presents conjugation between a pair of C═C bonds. This conjugation is more complete in the aromatic benzene molecule. The effects of substitution to the aromatic ring are considered by adding an external —OH group to form phenol, or by way of the N atoms in the heteroaromatic imidazole. Lastly, the fusion of a pair of aromatic rings, one of which is heteroaromatic, leads to the indole species. It should be noted that the benzene molecule serves as a model of the Phe residue in proteins; likewise, phenol, imidazole, and indole simulate Tyr, His, and Trp, respectively, so the results ought to have implications for noncovalent bonds within proteins.

COMPUTATIONAL METHODS

All calculations were carried out using the Gaussian 09 software package.[40] The MP2 method was applied in conjunction with the aug-cc-pVDZ basis set. This level of theory has been found to provide excellent results for these sorts of interactions.[41−51] The binding energies of the complexes were calculated as the differences in energy between the complex and the sum of the monomers in their optimized geometries, corrected for BSSE using the counterpoise procedure.[52] The potential energy surface of each heterodimer was thoroughly searched in order to find all minima, which had no imaginary frequencies. Dimers were examined via the natural bond order (NBO) procedure[53,54] embedded in the Gaussian program. Symmetry adapted perturbation theory (SAPT)[55,56] was carried out via the Molpro suite of programs.[57]

RESULTS

CHF_3 as a Proton Donor. The binding energy of complexes of CF_3H with the various π electron systems is reported in the first column of Table 1. In some cases, more than one minimum was obtained for a particular pair of monomers. Only the most stable complex of the CH···π variety is displayed in the table and in Figure 1. The energies and

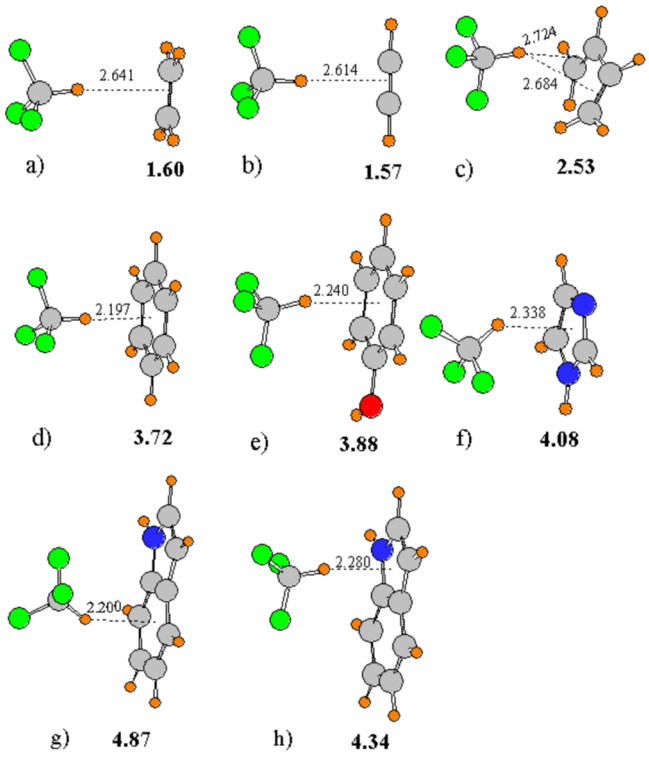

Figure 1. CH···π complexes of CHF_3 with various π donors. Distances in Å, and counterpoise-corrected binding energies (kcal/mol) displayed in bold.

structures of secondary minima are reported in Figure S1 of the Supporting Information. The proton of CF_3H approaches the π system of each electron donor, although not directly head-on in all cases. The reasons for these deviations are discussed in some detail below.

The interaction with the simple ethylene and acetylene is the weakest, with a binding energy of 1.6 kcal/mol. In the case of butadiene, the CF_3H proton is drawn toward the two terminal C—C bonds rather than to the central bond. This proclivity can be understood first on the basis of the normal Lewis structure of butadiene wherein it is the two terminal C═C

dx.doi.org/10.1021/jp5070598 | J. Phys. Chem. A 2014, 118, 9575−9587

bonds that involve a π-bond. This pattern is reinforced by the electrostatic potential which is most negative above these terminal C—C bonds, as illustrated in Figure 2c. The binding

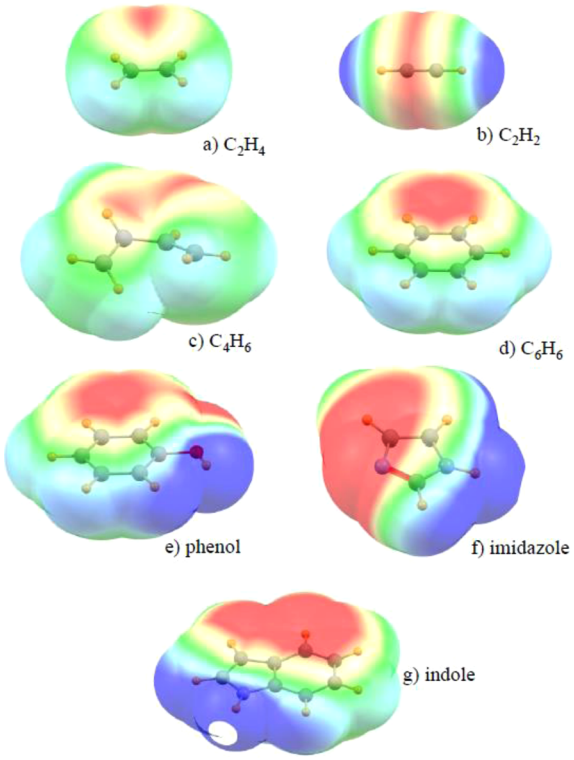

Figure 2. Electrostatic potentials on the surface corresponding to 2 × vdW radius. Red and blue colors indicate negative and positive regions, respectively. Maxima and minima correspond to ±0.02 au.

increases along with the size of the donor, up to 3.7 kcal/mol for benzene and 3.9 kcal/mol for phenol. This quantity rises above 4 kcal/mol when heteroatoms are added to the ring, as in imidazole and indole. The intensity of the negative electrostatic potential, indicated by the extent of the red regions in Figure 2, correlates nicely with the binding energy.

Turning next to phenol, the CH···π bond in Figure 1e is significantly distorted from linearity. The θ(CH···c) angle, where c refers to the center of the phenyl ring, is 147.8°. This bending presumably takes place in order to accommodate an electrostatic attraction between the negative potential around a F atom of CF_3H and the positive region around the OH group of phenol (see Figure 2e). One might have anticipated that a CH···O HB to the oxygen of phenol, or OH···F, ought to be stronger than the CH···π bond in Figure 1, but this is not the case. Figure S1 in the Supporting Information illustrates five secondary minima for the CF_3H/phenol complex. Structure a is quite similar to the global minimum, with a nearly equal binding energy, differing only in a slight rotation of the proton donor molecule about its C−H axis. Structure b is higher in energy, stabilized by a CH···O HB coupled with OH···F in a cyclic geometry. The CH···O HB appears again in c, and is replaced entirely by a OH···F HB in d. The highest energy dimer e contains no HB at all, with a binding energy of only 1.1 kcal/mol. In this particular pair of molecules, it would appear then that a CH···π HB is more stabilizing than CH···O or OH···F, either singly or in combination.

In the case of heterocyclic imidazole, the high basicity of N leads to an energetic preference for the CH···N over CH···π, especially as the former HB can be reinforced by a weaker CH···F as in f and g in Figure S1 (Supporting Information). The CH···π structure in Figure 1 has a binding energy of 4.1 kcal/mol, about 1 kcal/mol smaller than the two former minima. Note the angular distortion of the CH···π bond, with a θ(CH···c) angle of 134°. This angular distortion is again a result of electrostatic forces, since Figure 2f shows that the most positive region of the imidazole electrostatic potential surrounds the NH group, attracting the F atoms of the CF_3H. (Indeed, there are similar angular distortions present for all of the heterocyclic rings with θ(CH···c) between 134 and 149°.) Somewhat less stable are minima h and i in Figure S1 (Supporting Information), both of which contain NH···F HBs, followed finally by structure j with a binding energy of less than 1 kcal/mol, containing a single weak CH···F HB.

In connection with indole, note that there is a stronger interaction with its larger six-membered ring, although the N atom is located in the smaller ring. The electrostatic potential of Figure 2g helps explain this distinction, as there is a more intense and extensive negative potential above the larger ring. Without an unprotonated N atom as occurs in imidazole, indole cannot readily engage in a CH···N HB, leaving the CH···π interaction in Figure 1 as the dominating attractive force. A secondary minimum was found which contains a NH···F HB, but this structure lies some 3 kcal/mol higher in energy than the global minimum, and another wherein the CF_3H floats above the indole plane but with its CH turned away from the π-system.

It is frequently observed that the r(CH) bond undergoes a contraction when forming a CH···O HB, and that its stretching frequency is shifted to the blue, both of these patterns in contrast to trends in HBs in general. The first column of Table 2 shows that the CH bond of CF_3H fulfills this pattern, undergoing a small contraction upon formation of the CH···π complexes, on the order of 1−3 mÅ. Consistent with this contraction, the next column shows the CH stretching frequency is shifted to the blue. The largest of these changes

Table 2. Change of r(XH) (mÅ) and ν(CH) (cm^{-1}) Caused by Formation of CH/NH···π Complexes

proton acceptor	F_3CH, Δr	F_3CH, $\Delta\nu$	$N(CH_3)_3$, Δr	$N(CH_3)_4^+$, Δr	NH_4^+, Δr
ethylene	−0.8	10.9	−0.98, −0.98	−0.18, 0.06, 0.06	23
acetylene	−1.0	16.0	−0.6, −0.58, 0.52	−0.42, 0.08, 0.08	19
butadiene	−1.8	21.4	−1.8	−0.23, −0.13, 0.37	17, 1
benzene	−3.1	50.7	−3.96	−0.79, −0.08	14, 0
phenol	−1.9	29.5	−1.8, −0.95	−0.85, −0.49, −0.85	14, 0
imidazole	−0.5	9.7	−1.56, −1.3	−1.18, 0.17, 1.18	20, 0
indole	−0.7,[a] −1.9[b]	10.8,[a] 29.8[b]	−0.60, −0.56, −0.21	−1.15, −0.67	14, 5

[a]CH poised above 5-membered ring. [b]CH poised above 6-membered ring.

dx.doi.org/10.1021/jp5070598 | J. Phys. Chem. A 2014, 118, 9575−9587

is associated with benzene, with Δr(CH) = −3.1 mÅ and $\Delta\nu$(CH) = 51 cm^{-1}, even though benzene does not form the strongest CH···π bond. Likewise, imidazole induces the smallest shifts even though it represents one of the strongest CH···π complexes; changes for indole are also generally small. The largest changes for benzene may be associated with its near linear CH···π arrangement (see Table 1).

Another means of understanding the above trends emerges from NBO analysis. E(2) represents an estimate of the energy involved in a given charge transfer between two specific orbitals. For the CH···π complexes, there is a sizable transfer from the π orbitals of the unsaturated molecule to the σ^*(CH) antibonding orbital of CF_3H. These quantities are listed in Table 3, and are generally in the range between 2.3 and 4.1

Table 3. NBO Values of E(2) (kcal/mol) of CH···π and NH···π Complexes

proton acceptor	F_3CH	$N(CH_3)_3$	$N(CH_3)_4^+$	NH_4^+
ethylene	3.95	0.38[a]	3.72[b]	22.50
acetylene	3.45	0.49[c,d]	3.88[b]	20.13[c]
butadiene	2.28[c]	0.27	5.71[b,c]	18.66[a,c]
benzene	4.13[e]	1.29[c]	5.16[a,e]	12.68[a,e]
phenol	3.24[c]	2.16[a,c]	6.77[b,f]	12.37[a,e]
imidazole	3.37[c]	3.31[a,g]	7.50[h]	20.21[a,c]
indole	3.56,[c,i] 3.71[e,j]	1.94[e,b]	6.43[a,k]	13.26[b,e]

[a]Sum of charge transfer over two X−H σ^* orbitals. [b]Sum of charge transfer over three X−H σ^* orbitals. [c]Sum of two π orbitals. [d]Charge is transferred from CC π to C−N σ^* orbital. [e]Sum of three π orbitals. [f]Sum of three π orbitals and a lone pair. [g]Sum of two π orbitals and a lone pair. [h]5.32 kcal/mol from C−N bond orbitals plus 2.32 from N lone pairs. [i]CH poised above 5-membered ring. [j]CH poised above 6-membered ring. [k]Sum of four π orbitals.

kcal/mol, with the maximum occurring for benzene. This maximum coincides with the largest Δr(CH) and $\Delta\nu$(CH) in Table 2. Given that E(2) is dependent upon the overlap between the donor and acceptor orbitals, one may surmise that the smaller magnitudes of E(2) for the heterocyclic rings are likely due to the aforementioned angular distortions of the CH···π systems.

A partitioning of the total interaction energy into its component parts provides another window into the nature of the interaction. The SAPT components are listed in Table 4. In most cases, the electrostatic (ES) and dispersion (DISP) terms are comparable to one another, followed by a smaller but still significant induction (IND) energy. The exceptions are the simple ethylene and acetylene which have a disproportionately smaller dispersion contribution. Each of these components tends to grow in magnitude from the top to bottom of Table 4,

Table 4. SAPT Components of Interaction Energy (kcal/mol) of CH···π Complexes Containing F_3CH

proton acceptor	ES	EX	IND	DISP	EX-IND + EX-DISP
ethylene	−3.21	3.54	−1.60	−1.90	1.41
acetylene	−3.03	3.13	−1.30	−1.70	1.08
butadiene	−4.35	5.74	−2.84	−4.11	2.72
benzene	−5.30	7.09	−3.02	−5.15	2.63
phenol	−5.85	8.25	−3.99	−5.94	3.77
imidazole	−5.87	6.89	−3.09	−5.20	2.79
indole	−6.44	9.07	−4.23	−6.91	3.91

so they follow a trend much like the total interaction energy itself. One can thus characterize this set of CH···π bonds as containing roughly equal stabilization from Coulombic and dispersion attractions for the conjugated systems but with a smaller dispersion component for the simpler C_2H_n molecules.

Pictorial representations of electron redistributions offer a valuable window into the nature of noncovalent interactions. Such plots are generated as the difference in total electron density between the complex on one hand and the sum of densities of the individual monomers in the same locations. Figure 3a illustrates such a redistribution for the $F_3CH···C_2H_4$

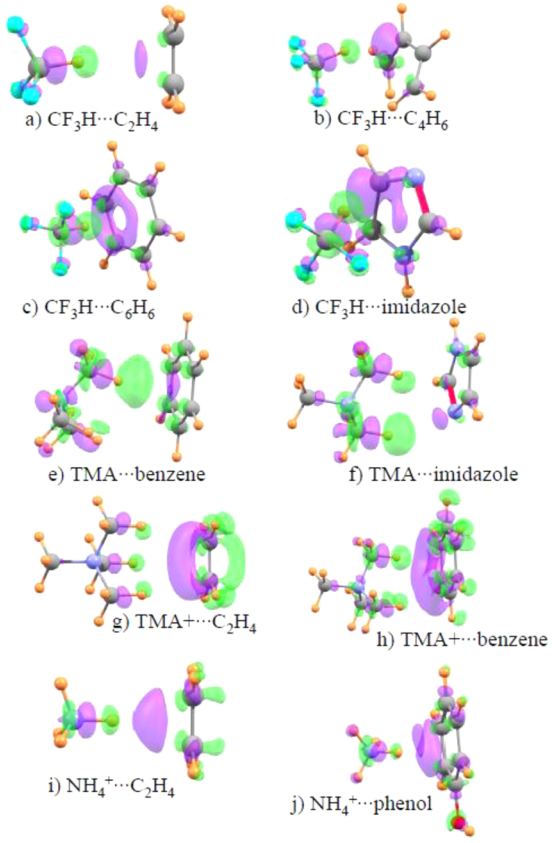

Figure 3. Electron density redistributions that accompany formation of the indicated complexes. Purple regions indicate density gain, and losses are green. Isocontours are ±0.0010 au for parts a−d, ±0.0004 for part e, ±0.0006 for part f, ±0.0010 for parts g and h, and ±0.0030 for parts i and j.

dimer, where green represents a loss of density upon formation of the complex and gains are indicated by purple. The green loss around the bridging proton is typical of H-bonds, and the H-bonding interaction with the ethylene π-system is verified by the purple density increase in that area. The diagram looks much the same for $F_3CH···C_2H_2$; this plot and others are presented in Figures S5−S8 in the Supporting Information. Whereas the distances in Figure 1 suggest that the proton ought to interact approximately equally with the two C═C bonds of butadiene, the density in Figure 3b indicates otherwise, that the interaction with one of these two bonds is much stronger. The equivalence of the six C—C bonds in benzene is manifest in the symmetry of the $F_3CH···$benzene redistribution diagram in Figure 3c, as is the case for phenol. This symmetry is broken in the case of imidazole, where it is the π-region above the unprotonated N atom and its

dx.doi.org/10.1021/jp5070598 | J. Phys. Chem. A 2014, 118, 9575−9587

neighboring two C atoms that exhibits the bulk of the purple density increase. The interaction with the 5-membered ring of indole involves the entire ring with the exception of the NH group, and the 6-membered ring resembles the benzene pattern.

$N(CH_3)_3$ Donor. Another potential CH donor arises when three methyl groups surround a central N atom. The electronegativity of the N imparts a certain level of acidity to the methyl groups, which are then capable of participating in CH···π HBs with π donors. On the other hand, the single N atom of trimethylamine (TMA) is not expected to match the three highly electronegative F atoms of CF_3H in terms of polarizing the CH bonds, so weaker CH···π interactions are anticipated. As an added issue, TMA permits the formation of multiple CH···π bonds simultaneously, involving protons either from a single methyl group or from several individual methyls. One can thus address the question of the relative strengths of a single CH···π bond as compared to several bent bonds of the same sort.

As may be noted by comparison of the first and third columns of Table 1, trimethylamine (TMA) forms somewhat weaker interactions with the various π-donors than does CF_3H. Given the presence of multiple CH donors on TMA, many of the minima are stabilized by more than one CH···π HB. In the case of acetylene, for example, Figure 4 show that three H atoms, all from the same methyl group, are attracted toward the π system, constituting a distorted trifurcated HB. (In fact, NBO analysis in Table 3 suggests this complex is stabilized not by CH···π HBs but rather by a transfer from the π orbitals of acetylene into the σ^*(CN) antibonding orbital.) Only slightly less stable is a similar configuration, except that each of the three H atoms is associated with a different methyl group. This structure is in fact stabilized purely by CH···π bonds, with no possibility of a $\pi \rightarrow \sigma^*$(CN) transfer. Of course, the N atom of TMA can serve as a strong proton-acceptor, so some of the most stable minima contain CH···N HBs. Acetylene is an example wherein the global minimum contains such a CH···N HB, as evident in Figure S2d (Supporting Information).

The minimum for ethylene is bifurcated in that the two CH groups of TMA interacting with the π system are spread apart such that one is above and the other is below the ethylene plane. This bifurcated arrangement is only very slightly more stable than the trifurcated structure, whether from a single or three separate methyl groups, illustrated in Figure S2 (Supporting Information). It might be noted that there are no local minima for either ethylene or acetylene which contain a single CH···π HB. The NBO values in Table 3 suggest that the charge transfer from the π orbitals into the σ^*(CH) antibonds is considerably smaller here than for CF_3H, even when all are summed together, suggesting very weak CH···π HBs, not only for ethylene and acetylene, but for most of these complexes as well.

Some of the symmetry is lost in the case of conjugated butadiene. The minimum shown in Figure 4c has a single CH···π HB, with a H···c distance of some 2.88 Å. This weak HB is supplemented by a small amount of transfer, from the butadiene π system to the σ^*(CN) antibond of TMA, a sort of tetrel bond. There are two other minima with similar energy, containing respectively 1 or 3 CH···π HBs. As in most of these cases, the global minimum for this pair is stabilized by a HB wherein the N lone pair acts as an electron donor, to a C−H bond in butadiene. There is a single CH···π HB in the global minimum of TMA with benzene, barely favored over the

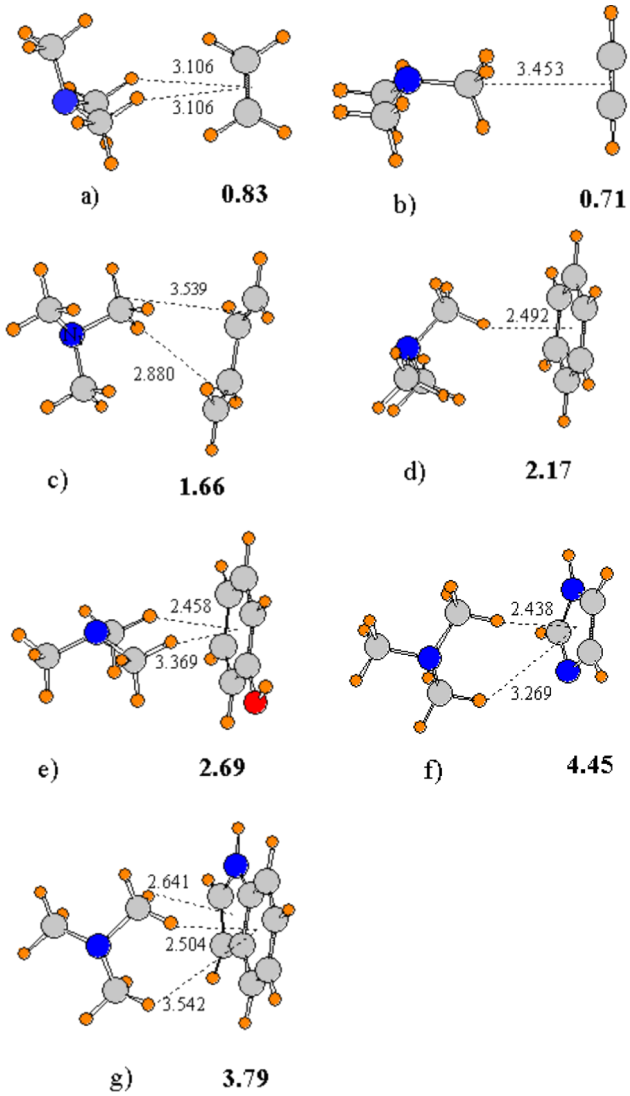

Figure 4. CH···π complexes of $N(CH_3)_3$ with various π donors. Distances in Å, and counterpoise-corrected binding energies (kcal/mol) displayed in bold.

approach of two or three separate CH groups toward the molecule's center, structures i and j in Figure S2 (Supporting Information). Another sort of structure, slightly less stable, has the N atom approach the benzene from above. There is no appreciable charge transfer here, and this geometry is probably stabilized primarily by a dipole−quadrupole interaction.

The OH···N HB is a strong interaction by its very nature, so it is not surprising that the global minimum of TMA with phenol contains such a bond. However, there are also a number of minima characterized by CH···π interactions, all with binding energies of 2.5−2.7 kcal/mol, depending upon whether there are one, two, or three such bonds. Just as the OH···N HB of phenol is a dominating interaction, so too is the very strong NH···N HB in which the NH of imidazole serves as a proton donor. However again, there are a number of stable minima containing CH···π HBs, the most stable of which is illustrated in Figure 4f as held together by a pair of CH···π HBs, as well as a CH···N interaction. This structure represents the most strongly bound such complex with TMA, with a binding energy of 4.5 kcal/mol, even more tightly held than another structure which contains three CH···N HBs (q in Figure S2, Supporting

dx.doi.org/10.1021/jp5070598 | J. Phys. Chem. A 2014, 118, 9575−9587

Information). As in the case of imidazole, the NH group of indole is also a potent proton donor, so it is not surprising to see a NH···N HB in the global minimum. With the exception of this structure, the most stable complex between TMA and indole includes two, or arguably three, CH···π HBs, spanning both rings.

In a molecule like TMA which has nine tightly coupled CH stretches, it is difficult to distinguish the CH stretching modes that correspond to H-bonded protons from those that do not. On the other hand, it is possible to consider any changes of individual CH bond lengths. The CH bonds participating in HBs are generally contracted relative to the isolated TMA monomer. These reductions vary from about 0.6 mÅ for acetylene and indole up to 4.0 mÅ for the single CH···π bond with benzene, as reported in Table 2. Again, it is emphasized that benzene has a combination of a strong CH···π bond and a nearly linear CH···c arrangement.

Results of SAPT dissection of the binding energy of the various complexes with TMA are reported in Table 5. Taking

Table 5. SAPT Components of Interaction Energy (kcal/mol) of CH···π Complexes Containing TMA

proton acceptor	ES	EX	IND	DISP	EX-IND + EX-DISP
ethylene	−0.82	2.56	−0.58	−2.95	0.85
acetylene	−0.99	2.40	−0.71	−2.15	0.97
butadiene	−2.03	5.22	−1.29	−5.07	1.84
benzene	−3.07	7.78	−2.57	−7.17	3.48
phenol	−3.24	8.34	−2.31	−7.71	3.11
imidazole	−3.38	7.09	−2.33	−6.14	2.70
indole	−4.46	10.60	−3.45	−9.94	4.64

benzene as an example, the electrostatic component of −5.3 kcal/mol for CF_3H is reduced to −3.1 kcal/mol for TMA; likewise for the induction energy, reduced from −3.0 to −2.6 kcal/mol. On the other hand, the dispersion term becomes more attractive, increasing from −5.2 to −7.2 kcal/mol. This pattern is in fact typical of the transition from CF_3H to TMA: reduced ES and IND but enhanced DISP. The net result is that the TMA complexes are bound primarily by dispersion, which is generally twice as large as ES, which is in turn larger than IND.

The CH···π HBs for TMA exhibit certain differences in electron density redistributions from those involving CF_3H. Whereas most HBs show roughly equal regions of loss around the proton and gain in the lone pair of the proton acceptor, the former losses outweigh the latter gains for TMA. The dominance of the green vs purple regions is exemplified in the cases of benzene and imidazole in Figure 3e and f, respectively. This pattern is common to all the complexes of TMA, as is evident in Figure S6 (Supporting Information).

$N(CH_3)_4^+$ Donor. The ability of a molecule to donate a proton is greatly enhanced by the presence of a positive charge. The tetramethylammonium $N(CH_3)_4^+$ species (TMA+) thus offers a means to isolate this enhancement for study by comparison with the very similar neutral $N(CH_3)_3$. The minima formed by this cation with the various π-systems are presented in Figure 5, from which it may first be noted that the CH···c distances are considerably shorter than those of the neutral analogues in Figure 4. For example, these HB distances are 3.1 Å for the complex of ethylene with TMA but shortened to 2.9 Å for TMA+. The energetic magnification of the binding

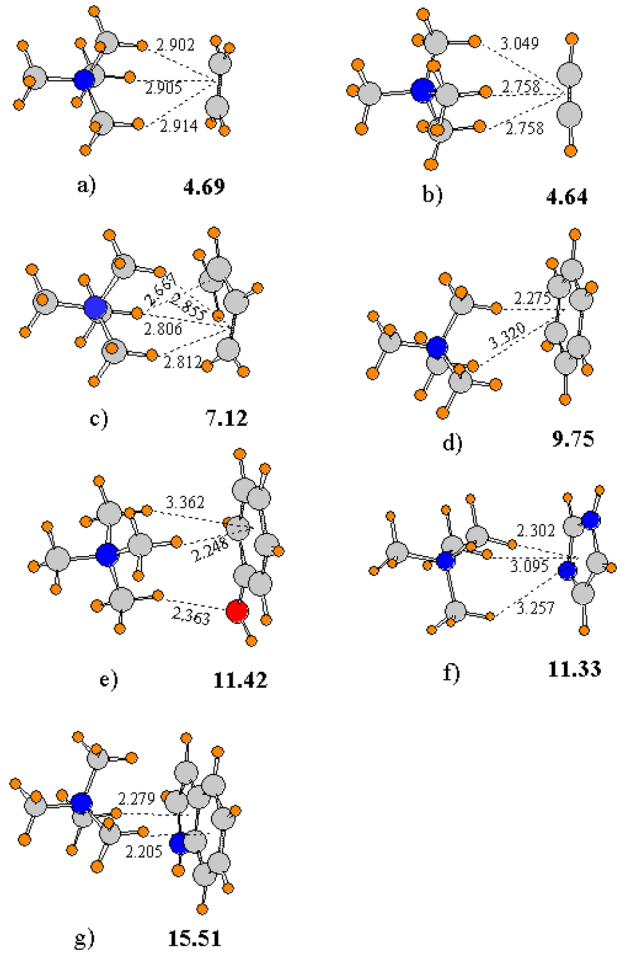

Figure 5. Complexes of $N(CH_3)_4^+$ with various π donors. Distances in Å, and counterpoise-corrected binding energies (kcal/mol) displayed in bold.

energies is even more dramatic in Table 1 where these quantities are 4−7 fold larger for TMA+. The values of 5−16 kcal/mol rank these CH···π HBs among some of the strongest noncovalent interactions in the literature.

In terms of geometry, both ethylene and acetylene engage in trifurcated CH···π HBs, although one of these three HBs is somewhat longer in the case of acetylene. Trifurcation involving three separate methyl groups is again preferred to participation of a single methyl group, as may be seen in Figure S3 (Supporting Information). The interaction with benzene is dominated by a single CH···π HB, rather short at 2.275 Å. The binding energy exceeds 10 kcal/mol for the other aromatic systems. The hydroxyl of phenol serves as a proton acceptor, rather than its role of donor for neutral TMA, supplementing the CH···π, and leading to a total binding energy of 11.4 kcal/mol. Note that the CH···c distance is shorter than R(CH···O) by 0.12 Å in the global minimum of Figure 5e. In the case of imidazole, the CH protons prefer to engage with the N lone pair rather than with imidazole's π system. Also, the electrostatic potential of imidazole is most negative in its molecular plane, serving as a powerful pull on the TMA+ cation. Consequently, the CH···π type structure in Figure 5 was optimized by forcing the TMA+ to remain above the Im plane; specifically, the N of TMA+ was held directly above the center of Im. Even so, the CH···π complex in Figure 5f is bound by 11.3 kcal/mol, with one CH···π interaction considerably

dx.doi.org/10.1021/jp5070598 | J. Phys. Chem. A 2014, 118, 9575−9587

stronger than the other two. There are a pair of CH···π HBs in the complex with indole, a single such bond to each of the two aromatic rings, and both shorter than 2.3 Å.

The stronger interactions involving TMA+ are reflected as well in the NBO charge transfer energies in Table 3. The values of E(2) for TMA+ are between 2 and 20 times larger than the same quantities for neutral TMA. A comparison of the effects of complexation on the C−H bond lengths for the neutral and cationic proton donors in Table 2 is intriguing and perhaps surprising. Despite the much greater strength of the interactions in the cationic dimers, these bonds undergo a generally smaller perturbation. As in their neutral counterparts, these bonds are usually but not always contracted. However, the degree of reduction is generally smaller for the cations. Taking ethylene as an example, r(CH) contracts by 1.0 mÅ when complexed with neutral TMA but by less than 0.2 mÅ with TMA+. The 4 mÅ contraction of TMA with benzene is reduced to less than 1 mÅ for TMA+.

The added charge enhances the electrostatic component of the interaction energy by a factor of 3−6, as is evident from a comparison of the SAPT data for TMA and TMA+ in Tables 5 and 6, respectively. There is a similar magnification of the induction energy. Dispersion also undergoes an increase albeit by not quite as dramatic of a factor. In general, these ionic CH···π complexes are bound by electrostatics and dispersion in roughly equal measure, with IND only slightly smaller.

Table 6. SAPT Components of Interaction Energy (kcal/mol) of CH···π Complexes Containing TMA+

proton acceptor	ES	EX	IND	DISP	EX-IND + EX-DISP
ethylene	−5.09	6.49	−4.13	−4.37	2.80
acetylene	−5.41	6.28	−3.62	−4.03	2.36
butadiene	−7.10	9.89	−5.85	−7.01	3.76
benzene	−9.34	12.58	−7.00	−8.95	4.62
phenol	−11.15	13.64	−7.42	−9.83	4.77
imidazole	−11.55	11.76	−3.09	−8.25	4.12
indole	−14.23	17.84	−9.55	−13.04	6.28

The density redistribution patterns for these ionic complexes look very much like those for typical HBs, including density loss around the bridging proton and gain in the region of the π-orbital donors, as exhibited in Figure S7 (Supporting Information). The purple gain region extends over the entire π system, whether just one C═C bond as in TMA+···C_2H_4 of Figure 3g or the full ring as in the case of larger π systems such as benzene (Figure 3h).

NH_4^+ Donor. NH_4^+ switches the proton donor atom from C to N while retaining the potency of a cationic proton donor. The effect of this switch upon the binding energy is evident in the comparison of the two final columns of Table 1, where NH_4^+ indeed forms tighter complexes, by roughly a factor of 2, than does TMA+. Indeed, the strongest complex examined in this entire study combines NH_4^+ with indole, with a binding energy of 25 kcal/mol. A single NH···π bond occurs for ethylene and acetylene, as indicated in Figure 6, but the interaction is of the bifurcated sort for the larger acceptor molecules, although one of the two NH···c HBs is typically significantly shorter and presumably stronger than the other.

The complex of NH_4^+ with benzene offers a comparison of the different possible modes of binding. The bifurcated arrangement is the global minimum, bound by 18.7 kcal/mol.

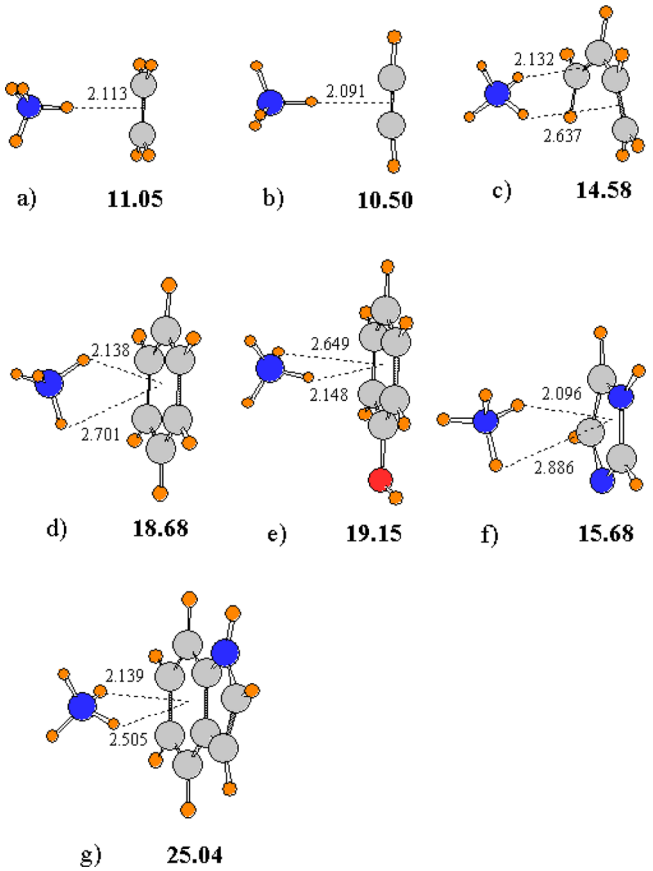

Figure 6. NH···π complexes of NH_4^+ with various π donors. Distances in Å, and counterpoise-corrected binding energies (kcal/mol) displayed in bold.

A single NH···π geometry is less stable, but by only 0.8 kcal/mol, and a trifurcated structure 0.6 kcal/mol higher still. It would appear then that there is nearly free rotation of the NH_4^+ cation above the benzene ring, a quasi-isotropic interaction potential. This behavior contrasts with that of the simpler ethylene π-system. In this case, NH_4^+ prefers a single NH···π bond, with a bifurcated structure less stable by 2.7 kcal/mol, followed closely by the trifurcated geometry; a similar pattern is noted for acetylene. As in the case of TMA+, the lone pair of the N atom of imidazole acts as a very strong draw on the NH_4^+ cation, so much so that the NH···π complex displayed in Figure 6 is not a true minimum, as it would decay to a NH···N type complex, where the ammonium lies in the imidazole plane. The structure in Figure 6f was obtained only by insisting that the ammonium N atom lie along the perpendicular of the imidazole plane, as was necessary for TMA+/imidazole.

The NH_4^+ cation behaves more like a classical HB donor than the various CH donors in a number of ways. Unlike the r(CH) contractions of the other systems, the NH bond elongates when participating in a HB. Table 2 shows that these stretches are of large magnitude, between 14 and 23 mÅ. The longest stretches are associated with the ethylene and acetylene complexes, likely due to the presence of only a single but linear NH···π bond. Also increased over the CH analogues are the charge transfer stabilization energies E(2) which climb to as high as 23 kcal/mol. Note that the latter value is associated with the complex of NH_4^+ with ethylene, one of the weakest interactions with this cation, but again one which is characterized by a single, linear NH···π HB. The NBO values

dx.doi.org/10.1021/jp5070598 | J. Phys. Chem. A 2014, 118, 9575−9587

of E(2) are also disproportionately raised in the NH···π complexes, as compared to CH···π, as is evident in the last column of Table 3.

The SAPT dissection of these ionic NH···π complexes in Table 7 points to induction and electrostatics as the prime

Table 7. SAPT Components of Interaction Energy (kcal/mol) of NH···π Complexes Containing NH_4^+

proton acceptor	ES	EX	IND	DISP	EX-IND + EX-DISP
ethylene	−11.89	12.79	−14.10	−3.65	7.56
acetylene	−11.70	11.18	−12.18	−3.33	6.10
butadiene	−14.25	15.02	−16.19	−5.30	7.50
benzene	−15.78	15.61	−16.60	−6.51	6.67
phenol	−16.13	16.27	−17.27	−6.76	7.03
imidazole	−13.60	14.64	−14.98	−5.95	6.04
indole	−20.96	19.23	−20.56	−7.98	8.45

contributing factors, with dispersion playing a smaller but certainly not insignificant role. A comparison with the data in Table 6 shows that the transition from ionic CH···π to NH···π raises both the ES and IND components but has the reverse effect of a small diminution in the dispersion contribution.

The electron redistribution patterns in these HBs (see Figure 3i and j and Figure S8, Supporting Information) look much like those for typical HBs with a green loss region surrounding the bridging proton and purple gain in the area of the π system of the electron donor. It is interesting to note a pattern of patterns, as it were. Specifically, as the HB gains strength, progressing from TMA as the weakest proton donor to NH_4^+ as the strongest, the loss around the proton diminishes while the gain in the π system expands.

NMR Chemical Shifts. Whether red -shifting, as are most conventional HBs, or blue-shifting, which is true of many CH···O HBs, the NMR chemical shifts of the bridging protons[58−64] appear to make no distinction of that sort. Formation of a HB robs this proton of some of its surrounding electron cloud, and thus reduces its chemical shielding. The change in this chemical shielding is reported in Table 8 for the bridging proton in each complex. Focusing first on the simple systems in the first two rows, the loss of shielding is evident by the negative values of $\Delta\sigma$. The magnitude of this change is roughly proportional to the strength of the HB, smallest for TMA and largest for the NH···π HBs of NH_4^+. The situation is somewhat different for butadiene which exhibits no change for CF_3H and a very small positive change for TMA; the two cationic proton donors show the expected deshielding.

The values in the last four rows of Table 8 are all positive. This distinction is easily explained by the ring currents within these four aromatic systems, which produce a magnetic field that effectively shields any atom poised above their center. (Similar trends were observed earlier[64] in the case of OH···π interactions.) The value of $\Delta\sigma$ varies between 3.1 and 4.6 ppm for CF_3H, and is not simply related to the binding energy. The values for TMA are somewhat smaller, in the 2.6−3.3 ppm range, but again not directly proportional to ΔE; TMA+ shifts are comparable to those of CF_3H, even though the binding energies of the former are much greater. The shifts for the very strongly bound complexes of NH_4^+ with the aromatic systems are positive but only barely so.

One interpretation of these trends rests on two opposing effects. On one hand, formation of the HB pulls density away from the bridging proton, tending to make σ smaller. However, its presence above an aromatic system and its accompanying ring currents push σ in the opposite direction. The latter shielding effect wins out in most cases, so $\Delta\sigma$ is positive. However, the very strong deshielding of NH···π HBs for NH_4^+ more effectively counters the effects of aromatic ring currents, and a smaller positive value of $\Delta\sigma$ ensues. Indeed, examination of density shift maps like those in Figure 3 reinforces the idea of greater loss of electron density around the bridging proton of NH_4^+ than of the other donors.

SUMMARY AND DISCUSSION

The interactions with the various π-donors follow a pattern in that TMA is the weakest proton donor, followed in order by CF_3H, and then by the two ions TMA+ and NH_4^+. This pattern may be visualized via Figure 7 which displays the binding energies of the various complexes. The much stronger binding of the cations, and of NH_4^+ in particular, is plainly evident. It is also clear that there is a relatively small margin between F_3CH and TMA, less than 2 kcal/mol.

This order may be understood to some degree on the basis of electrostatic potentials, illustrated in Figure 8. The potentials range between +0.03 (blue) and −0.03 (red) for the two neutrals in a and b, where it is clearly evident that the potential around the CH in CF_3H is considerably more positive than the same areas in TMA. With respect to the two cations, the potential is positive in all directions, so the contours shown vary between +0.15 and +0.22 au. It is clear that the blue positive region is more intense around the protons of NH_4^+.

Comparison of the various contributors to the total interaction energies in Tables 4−7 also reveals some interesting trends. Consistent with the electrostatic potentials, the ES contribution rises steadily as TMA < CF_3H < TMA+ < NH_4^+. Not surprisingly, the IND energy follows a similar trend. The dispersion energy, however, is different. First, with respect to the two neutral proton donors, there is more dispersion energy in complexes of TMA than with CF_3H. Another reversal occurs in the two cations, where TMA+ DISP is larger than the same

Table 8. Change in Isotropic NMR Shielding, $\Delta\sigma$ (ppm), of Bridging Hydrogens Occurring upon Formation of a Complex

proton acceptor	CHF_3	$N(CH_3)_3$	$N^+(CH_3)_4$	NH_4^+
ethylene	−0.67	−0.27, −0.27	−0.54, −0.70, −0.55	−4.98
acetylene	−0.85	−0.08, −0.08, 0.05	−1.05, −1.00, −0.40	−4.97
butadiene	0.00	0.18	−0.34, −0.90, −0.66	−4.64, −1.58
benzene	4.44	2.70	−0.23, 3.37	0.62, 0.53
phenol	3.80	2.72, 0.35	3.29, −0.7, −0.39	0.03, 0.34
imidazole	3.07	2.63, −0.4	−0.25, −1.3, 3.22	−0.3, 0.53
indole	3.86,[a] 4.64[b]	2.94, 3.29, 0.43	−0.21, 4.01, 3.48	1.18, 1.41

[a]Poised over five membered ring. [b]Poised over six membered ring.

dx.doi.org/10.1021/jp5070598 | J. Phys. Chem. A 2014, 118, 9575−9587

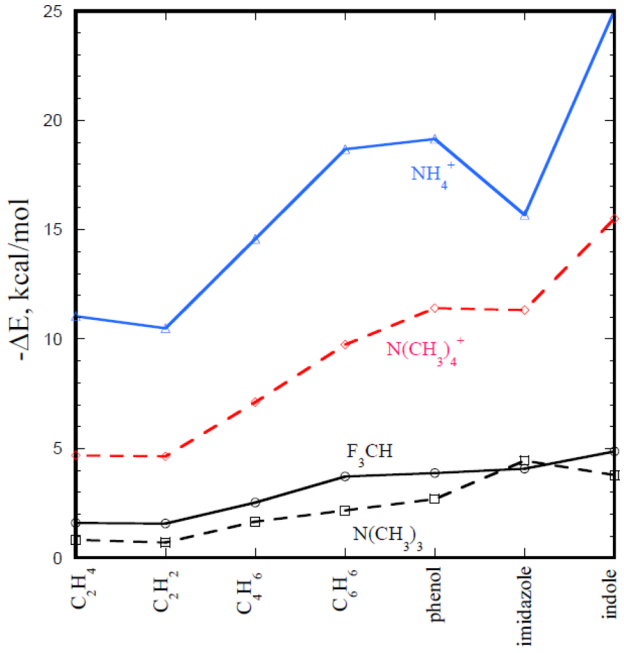

Figure 7. Binding energies for the various dimers.

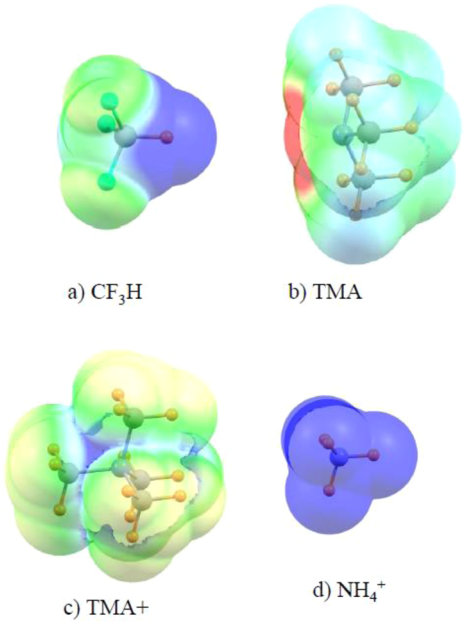

Figure 8. Electrostatic potentials lying on the surface corresponding to 1.5 × vdW radius. Colors correspond to +0.03 (blue) and −0.03 au (red) for the neutral molecules in parts a and b and +0.22 and +0.15 for the cations in parts c and d.

quantity for NH_4^+. In fact, the dispersion associated with the neutral TMA complexes is comparable to, and even larger than, the NH_4^+ dispersion energy. The disproportionately larger DISP in the TMA and TMA+ complexes may be due to the larger size of these two monomers, when compared to CF_3H and NH_4^+. Consequently, it is imperative that any computational study of complexes such as these include accurate assessment of dispersion energy, since it is comparable in magnitude, and sometimes even larger than ES or IND.

Despite its importance to the bonding, the NBO values of E(2) for $\pi \rightarrow \sigma^*$(CH) transfer are not a quantitative indicator of the total binding energy. For example, E(2) values for the TMA+ complexes are only slightly larger than the same quantities for F_3CH, even though the binding of the former is considerably stronger (see Figure 7). Also, even though TMA binds to the π systems almost as strongly as does F_3CH, E(2) of the former is much smaller, almost an order of magnitude smaller in some cases, than for the latter. Neither does E(2) accurately reflect the induction component of the interaction energy. Again, in a comparison between F_3CH and TMA, IND is only slightly smaller for the latter but E(2) is much smaller.

One final point about E(2) concerns its evaluation via localized NBO orbitals. As such, the π-system of an aromatic molecule like benzene is represented by three separate C═C bonds, rather than the fully delocalized picture. The NBO charge transfer from benzene thus arises from these three C═C bonds, each of which overlaps with the σ^*(CH) antibond. In the canonical delocalized picture, the only occupied π-orbital that is not orthogonal to σ^*(CH) is the lowest-energy symmetric one, which could make the equivalent transfer of charge.

Complexation causes changes in the C−H and N−H bond lengths. The latter grows longer, as is typical of most HBs. The CH bond, on the other hand, contracts. This shortening is of larger magnitude for the weaker CH···π bonds involving F_3CH and TMA, whereas the bond contraction is smaller for the TMA+ cation, less than 1 mÅ. Given the observation that charge is being transferred into the σ^* antibonding CH orbital, the contraction of this bond might seem puzzling at first glance. However, it must be remembered that these bond length changes are the product of more than one factor. In addition to this charge transfer/hyperpolarization, rehybridization of the CH bonding orbital must be considered as well. A decrease of the p vs s contribution would tend to shorten the bond in question, according to Bent's rule.[65−69]

Indeed, the first column of Table 9 illustrates that such a diminution of p-contribution occurs for F_3CH. These changes are large enough to overshadow the modest bond-lengthening values of E(2) in Table 3, and the result is a bond contraction. These rehybridizations are displayed as the broken blue line in Figure 9. Opposing these contractions are bond-lengthening charge transfers into the σ^*(CH) antibonding orbital, illustrated in Figure 9 as the solid red curve. The combination of these two factors is chiefly responsible for the observed changes in the CH bond length, indicated by the solid black curve. It may be noted that the blue rehybridization curve more closely mimics the pattern of Δr. The rehybridizations of the NH bonding orbital in the NH_4^+ complexes are even larger in magnitude, as evident in the last column of Table 9. However,

Table 9. Change in %p Character of C sp^x Hybrid as Part of the C−H or N−H Bond of CH···π and NH···π Complexes

proton acceptor	F_3CH	NH_4^+
ethylene	−0.78	−4.31
acetylene	−0.75	−4.01
butadiene	−0.89	−3.05
benzene	−1.76	−3.27
phenol	−1.57	−2.99
imidazole	−1.32	−3.80
indole	−1.41,[a] −1.74[b]	−2.42

[a]CH poised above 5-membered ring. [b]CH poised above 6-membered ring.

dx.doi.org/10.1021/jp5070598 | J. Phys. Chem. A 2014, 118, 9575−9587

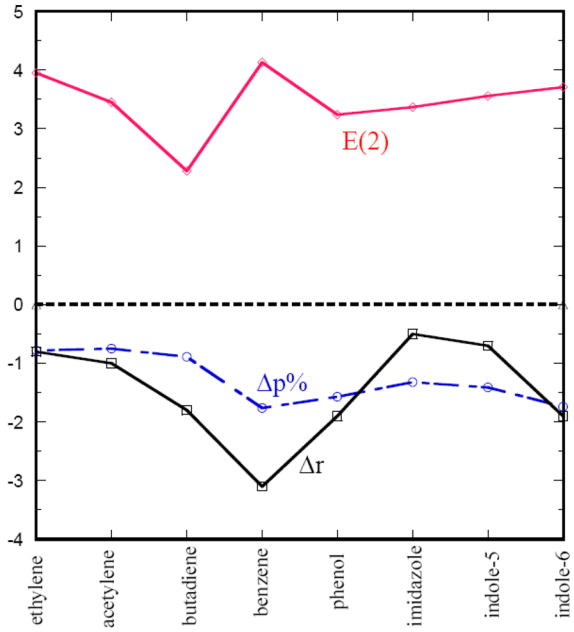

Figure 9. Values of properties upon formation of a complex of F_3CH with each indicated proton acceptor. Δr represents the change in C−H bond length in mÅ, E(2) refers to charge transfer into the σ^*(CH) antibond in kcal/mol, and Δp% represents the change in the p-orbital percentage contribution to the C−H bonding orbital.

even these quantities are overwhelmed by the very substantial values of E(2), between 13 and 22 kcal/mol, leading to the NH bond lengthening. Between these two extremes lies $N(CH_3)_4^+$ where the two forces are more nearly balanced and only small changes in bond length are observed.

Earlier work[33] had considered the manner in which adding a positive charge can affect the magnitude of the binding of a methyl amine to a lone pair. Specifically, taking TMA as a sample neutral amine, the most stable structure contained a trifurcated CH···O HB to the carbonyl O atom of *N*-methylacetamide (NMA). The two molecules were bound by 2.1 kcal/mol. This quantity exceeds the binding energy of the same TMA to the π-systems of ethylene, acetylene, and butadiene. However, the CH···π bonds are stronger than CH···O when they engage the aromatic π-systems benzene, phenol, imidazole, and indole. Adding a positive charge to the amine, i.e., changing TMA to TMA+, had magnified by 9-fold the CH···O HB to NMA, bringing the binding energy up to 18.8 kcal/mol. The charge-induced magnification of the CH···π bonds is again strong but not quite as dramatic, raising the binding energy of the various complexes by a factor of 4−7. Consequently, even the strongest complexes pictured in Figure 5 are not quite as strong as the one between $N(CH_3)_4^+$ and the O lone pairs of NMA. Comparison of NBO values of E(2) suggests a greater degree of charge transfer stabilization for O lone pairs as compared to π-systems. Whether a lone pair or π-system electron donor, dispersion plays the largest role in binding of the neutral pairs. The situation is different for the ionic pairs: Whereas electrostatic attraction dominates for lone pair donors, it shares nearly equally with induction and dispersion for π-system donors.

There are some data in the literature with which certain of our results can be compared. First, with respect to charged systems, experimental measurements[70] of the binding enthalpy of NH_4^+ with benzene and ethylene are equal to 19.3 and 10.0 kcal/mol, respectively. These values compare very well with our corresponding calculated binding energies of 18.7 and 11.0 kcal/mol. ΔH for the TMA+/benzene interaction[71] is 9.4 kcal/mol, also in good agreement with our calculated ΔE of 9.8 kcal/mol.

There are some earlier calculated data on charged systems as well, primarily computed at the MP2 level with various basis sets. The best of these, 6-311+G** calculations[72,73] yielded binding energies of 8.7 and 16.9 kcal/mol for the complexes of benzene with TMA+ and NH_4^+, a bit weaker binding than our own results with the larger aug-cc-pVDZ, 9.8 and 18.7 kcal/mol, respectively. The TMA+/benzene dimer was bound by only 7.5 kcal/mol with 6-31+G**.[74] A smaller 6-31G** basis[75] found a TMA+/benzene binding energy of 9.1 kcal/mol. These lesser quantities are consistent with the importance of dispersion, which is typically saturated only with large basis sets such as the aug-cc-pVnZ series. This same study[75] computed the binding energy of TMA+ with imidazole to be 16.3 kcal/mol, nearly coincident with a 6-31+G** estimate[76] of 16.4 kcal/mol, both only slightly less than our own value of 16.8 kcal/mol. With respect to the $NH^+\cdots\pi$ bond, a recent CCSD(T) computation[77] arrived at a NH_4^+/benzene binding energy within 2% of our own MP2 result, and confirms the small energy difference between mono, bi, and tridentate structures.

Turning next to neutral dimers, a high-level calculation has been carried out for the neutral $CF_3H\cdots$benzene pair[78] which shows that going beyond MP2 to CCSD(T) and extending to the basis set limit adds only a small increment (0.5 kcal/mol) to the binding energy obtained here. The chlorosubstituted version of F_3CH binds to benzene by 5.5 kcal/mol in a very high level CCSD(T) calculation at the basis set limit.[79] This 1.4 kcal/mol increment of Cl_3CH over F_3CH is consistent with an earlier work.[78] Further, the calculated geometry matches nicely with a recent microwave structure,[80] which also supports our finding that the aromatic benzene molecule binds more strongly to this proton donor than do simple double or triple CC bonds. In the case of another but related system, the CH···π HB in NCH···benzene was computed[81] to have a binding energy of 4.6 kcal/mol with a cc-pVTZ basis, slightly larger than our value of 3.7 kcal/mol for F_3CH, consistent with the greater acidity of the former.

In summary, while normally weak, there are a number of means by which CH···π HBs can be strengthened. First, with respect to the electron donor, there is a trend of increasing HB strength as the simple C═C bond of ethylene or acetylene is conjugated, as in butadiene. The aromaticity of benzene enhances the binding, which is further enhanced by a —OH substituent as in phenol, with even greater effects arising in the heteroaromatic imidazole or indole. Adding electron-withdrawing agents to the proton donor molecule, as in CF_3H, amplifies its proton-donating power, to the point where CH···π HBs are comparable to standard OH···O HBs as in the water dimer, for example. Even the weaker proton donor of trimethylamine can form fairly strong HBs, particularly with the heteroaromatic imidazole and indole. However, the most effective means of strengthening a CH···π HB is the addition of positive charge to the donor. The binding energy of tetramethylammonium cation to any π-system is very strong indeed, varying from 4.7 kcal/mol for the simple ethylene or acetylene, up to 9.8 kcal/mol for the prototypical aromatic benzene, and as high as 15.5 kcal/mol for indole. There is no single source of the strength of these HBs, which owe their

dx.doi.org/10.1021/jp5070598 | J. Phys. Chem. A 2014, 118, 9575−9587

binding to a combination of electrostatic, induction, and dispersion attraction.

■ ASSOCIATED CONTENT

Supporting Information

Full refs 5, 40, 57, and 61 as well as the geometries and binding energies of secondary minima and the electronic redistribution patterns of all complexes. This material is available free of charge via the Internet at http://pubs.acs.org.

■ AUTHOR INFORMATION

Corresponding Author

*E-mail: steve.scheiner@usu.edu.

Notes

The authors declare no competing financial interest.

■ ACKNOWLEDGMENTS

This work has been supported by NSF-CHE-1026826. Computer, storage, and other resources from the Division of Research Computing in the Office of Research and Graduate Studies at Utah State University and the CTI (CSIC) are gratefully acknowledged.

■ REFERENCES

(1) Müller-Dethlefs, K.; Hobza, P. Noncovalent Interactions: A Challenge for Experiment and Theory. *Chem. Rev.* **2000**, *100*, 143−167.

(2) Johnson, E. R.; Keinan, S.; Mori-Sanchez, P.; Contreras-Garcia, J.; Cohen, A. J.; Yang, W. Revealing Noncovalent Interactions. *J. Am. Chem. Soc.* **2010**, *132*, 6498−6506.

(3) Scheiner, S. *Hydrogen Bonding. A Theoretical Perspective*; Oxford University Press: New York, 1997; p 375.

(4) Gilli, G.; Gilli, P. *The Nature of the Hydrogen Bond*; Oxford University Press: Oxford, U.K., 2009; p 313.

(5) Arunan, E.; Desiraju, G. R.; Klein, R. A.; Sadlej, J.; Scheiner, S.; Alkorta, I.; Clary, D. C.; Crabtree, R. H.; Dannenberg, J. J.; Hobza.; et al. Definition of the Hydrogen Bond. *Pure Appl. Chem.* **2011**, *83*, 1637−1641.

(6) Biswal, H. S.; Gloaguen, E.; Loquais, Y.; Tardivel, B.; Mons, M. Strength of NH···S Hydrogen Bonds in Methionine Residues Revealed by Gas-Phase IR/UV Spectroscopy. *J. Phys. Chem. Lett.* **2012**, *3*, 755−759.

(7) Solimannejad, M.; Scheiner, S. Unconventional H-Bonds: SH···N Interaction. *Int. J. Quantum Chem.* **2011**, *111*, 3196−3200.

(8) Chalasinski, G.; Cybulski, S. M.; Szczesniak, M. M.; Scheiner, S. Nonadditive Effects in HF and HCl Trimers. *J. Chem. Phys.* **1989**, *91*, 7048−7056.

(9) Latajka, Z.; Scheiner, S. Structure, Energetics and Vibrational Spectrum of H_2O-HCl. *J. Chem. Phys.* **1987**, *87*, 5928−5936.

(10) Cybulski, S.; Scheiner, S. Hydrogen Bonding and Proton Transfers Involving Triply Bonded Atoms. HC≡N and HC≡CH. *J. Am. Chem. Soc.* **1987**, *109*, 4199−4206.

(11) Zierke, M.; Smieško, M.; Rabbani, S.; Aeschbacher, T.; Cutting, B.; Allain, F. H.-T.; Schubert, M.; Ernst, B. Stabilization of Branched Oligosaccharides: Lewis Benefits from a Nonconventional C−H···O Hydrogen Bond. *J. Am. Chem. Soc.* **2013**, *135*, 13464−13472.

(12) Horowitz, S.; Dirk, L. M. A.; Yesselman, J. D.; Nimtz, J. S.; Adhikari, U.; Mehl, R. A.; Scheiner, S.; Houtz, R. L.; Al-Hashimi, H. M.; Trievel, R. C. Conservation and Functional Importance of Carbon-Oxygen Hydrogen Bonding in Adomet-Dependent Methyltransferases. *J. Am. Chem. Soc.* **2013**, *135*, 15536−15548.

(13) Yang, H.; Wong, M. W. Oxyanion Hole Stabilization by C-H···O Interaction in a Transition State-a Three-Point Interaction Model for Cinchona Alkaloid-Catalyzed Asymmetric Methanolysis of Meso-Cyclic Anhydrides. *J. Am. Chem. Soc.* **2013**, *135*, 5808−5818.

(14) Scheiner, S. Contribution of CH··X Hydrogen Bonds to Biomolecular Structure. In *Hydrogen Bonding - New Insights*; Grabowski, S. J., Ed.; Springer: Dordrecht, 2006; pp 263−292.

(15) Jones, C. R.; Baruah, P. K.; Thompson, A. L.; Scheiner, S.; Smith, M. D. Can a C-H···O Interaction Be a Determinant of Conformation. *J. Am. Chem. Soc.* **2012**, *134*, 12064−12071.

(16) Scheiner, S. Weak H-Bonds. Comparisons of CH···O to NH···O in Proteins and PH···N to Direct P···N Interactions. *Phys. Chem. Chem. Phys.* **2011**, *13*, 13860−13872.

(17) Scheiner, S. Relative Strengths of NH··O and CH··O Hydrogen Bonds between Polypeptide Chain Segments. *J. Phys. Chem. B* **2005**, *109*, 16132−16141.

(18) Gu, Y.; Kar, T.; Scheiner, S. Comparison of the CH···N and CH···O Interactions Involving Substituted Alkanes. *J. Mol. Struct.* **2000**, *552*, 17−31.

(19) Nishio, M.; Umezawa, Y.; Fantini, J.; Weiss, M. S.; Chakrabarti, P. CH−π Hydrogen Bonds in Biological Macromolecules. *Phys. Chem. Chem. Phys.* **2014**, *16*, 12648−12683.

(20) Takahashi, O.; Kohno, Y.; Saito, K. Molecular Orbital Calculations of the Substituent Effect on Intermolecular CH/π Interaction in C_2H_3X–C_6H_6 Complexes (X=H, F, Cl, Br, and OH). *Chem. Phys. Lett.* **2013**, *378*, 509−515.

(21) Bloom, J. W. G.; Raju, R. K.; Wheeler, S. E. Physical Nature of Substituent Effects in XH/π Interactions. *J. Chem. Theory Comput.* **2012**, *8*, 3167−3174.

(22) Kumar, S.; Mukherjee, A.; Das, A. Structure of Indole··· Imidazole Heterodimer in a Supersonic Jet: A Gas Phase Study on the Interaction between the Aromatic Side Chains of Tryptophan and Histidine Residues in Proteins. *J. Phys. Chem. A* **2012**, *116*, 11573−11580.

(23) Ramirez-Gualito, K.; Alonso-Rios, R.; Quiroz-Garcia, B.; Rojas-Aguilar, A.; Diaz, D.; Jimenez-Barbero, J.; Cuevas, G. Enthalpic Nature of the CH/π Interaction Involved in the Recognition of Carbohydrates by Aromatic Compounds, Confirmed by a Novel Interplay of NMR, Calorimetry, and Theoretical Calculations. *J. Am. Chem. Soc.* **2009**, *131*, 18129−18138.

(24) Brandl, M.; Weiss, M. S.; Jabs, A.; Sühnel, J.; Hilgenfeld, R. C-H···π-Interactions in Proteins. *J. Mol. Biol.* **2001**, *307*, 357−377.

(25) Ringer, A. L.; Figgs, M. S.; Sinnokrot, M. O.; Sherrill, C. D. Aliphatic C-H/π Interactions: Methane-Benzene, Methane-Phenol, and Methane-Indole Complexes. *J. Phys. Chem. A* **2006**, *110*, 10822−10828.

(26) Karthikeyan, S.; Ramanathan, V.; Mishra, B. K. Influence of the Substituents on the CH···π Interaction: Benzene−Methane Complex. *J. Phys. Chem. A* **2013**, *117*, 6687−6694.

(27) Ma, J. C.; Dougherty, D. A. The Cation-π Interaction. *Chem. Rev.* **1997**, *97*, 1303−1324.

(28) Meot-Ner, M. Update 1 of Strong Ionic Hydrogen Bonds. *Chem. Rev.* **2012**, *112*, pr22−pr103.

(29) Scheiner, S.; Wang, L. Hydrogen Bonding and Proton Transfers of the Amide Group. *J. Am. Chem. Soc.* **1993**, *115*, 1958−1963.

(30) Cybulski, S. M.; Scheiner, S. Comparison of Morokuma and Perturbation Theory Approaches to Decomposition of Interaction Energy. $(NH_4)^+$...NH_3. *Chem. Phys. Lett.* **1990**, *166*, 57−64.

(31) Scheiner, S.; Redfern, P.; Szczesniak, M. M. Effects of External Ions on the Energetics of Proton Transfers across Hydrogen Bonds. *J. Phys. Chem.* **1985**, *89*, 262−266.

(32) Cannizzaro, C. E.; Houk, K. N. Magnitude and Chemical Consequences of R_3N^+-C-H···O=C Hydrogen Bonding. *J. Am. Chem. Soc.* **2002**, *124*, 7163−7169.

(33) Adhikari, U.; Scheiner, S. The Magnitude and Mechanism of Charge Enhancement of CH··O H-Bonds. *J. Phys. Chem. A* **2013**, *117*, 10551−10562.

(34) Forman, J. E.; Barrans, R. E.; Dougherty, D. A. Circular Dichroism Studies of Molecular Recognition with Cyclophane Hosts in Aqueous Media. *J. Am. Chem. Soc.* **1995**, *117*, 9213−9228.

(35) Gromiha, M. M. Influence of Cation−π Interactions in Different Folding Types of Membrane Proteins. *Biophys. Chem.* **2003**, *103*, 251−258.

(36) Torrice, M. M.; Bower, K. S.; Lester, H. A.; Dougherty, D. A. Probing the Role of the Cation−π Interaction in the Binding Sites of GPCRs Using Unnatural Amino Acids. *Proc. Natl. Acad. Sci. U.S.A.* **2009**, *106*, 11919−11924.
(37) Yamada, S.; Iwaoka, A.; Fujita, Y.; Tsuzuki, S. Tetraalkylammonium-Templated Stereoselective Norrish−Yang Cyclization. *Org. Lett.* **2013**, *15*, 5994−5997.
(38) Dupont, J.; Suarez, P. A. Z.; Souza, R. F. D.; Burrow, R. A.; Kintzinger, J.-P. C-H-π Interactions in 1-n-Butyl-3-Methylimidazolium Tetraphenylborate Molten Salt: Solid and Solution Structures. *Chem.—Eur. J.* **2000**, *6*, 2377−2381.
(39) Gallivan, J. P.; Dougherty, D. A. Cation-π Interactions in Structural Biology. *Proc. Natl. Acad. Sci. U.S.A.* **1999**, *96*, 9459−9464.
(40) Frisch, M. J.; Trucks, G. W.; Schlegel, H. B.; Scuseria, G. E.; Robb, M. A.; Cheeseman, J. R.; Scalmani, G.; Barone, V.; Mennucci, B.; Petersson, G. A.; et al. *Gaussian 09*, revision B.01; Gaussian, Inc.: Wallingford, CT, 2009.
(41) Lu, N.; Ley, R. M.; Cotton, C. E.; Chung, W.-C.; Francisco, J. S.; Negishi, E.-I. Molecular Tuning of the Closed Shell C−H···F−C Hydrogen Bond. *J. Phys. Chem. A* **2013**, *117*, 8256−8262.
(42) Hauchecorne, D.; Herrebout, W. A. Experimental Characterization of C−X···Y−C (X = Br, I; Y = F, Cl) Halogen−Halogen Bonds. *J. Phys. Chem. A* **2013**, *117*, 11548−11557.
(43) Li, H.; Lu, Y.; Liu, Y.; Zhu, X.; Liu, H.; Zhu, W. Interplay between Halogen Bonds and $\pi-\pi$ Stacking Interactions: CSD Search and Theoretical Study. *Phys. Chem. Chem. Phys.* **2012**, *14*, 9948−9955.
(44) Azofra, L. M.; Scheiner, S. Substituent Effects in the Noncovalent Bonding of SO_2 to Molecules Containing a Carbonyl Group. The Dominating Role of the Chalcogen Bond. *J. Phys. Chem. A* **2014**, *118*, 3835−3845.
(45) Esrafili, M. D.; Fatehi, P.; Solimannejad, M. Mutual Interplay between Pnicogen Bond and Dihydrogen Bond in HMH···HCN···PH_2X Complexes (M = Be, Mg, Zn; X = H, F, Cl). *Comput. Theor. Chem.* **2014**, *1034*, 1−6.
(46) Adhikari, U.; Scheiner, S. Effects of Charge and Substituent on the S···N Chalcogen Bond. *J. Phys. Chem. A* **2014**, *118*, 3183−3192.
(47) Kerdawy, A. E.; Murray, J. S.; Politzer, P.; Bleiziffer, P.; Heßelmann, A.; Görling, A.; Clark, T. Directional Noncovalent Interactions: Repulsion and Dispersion. *J. Chem. Theory Comput.* **2013**, *9*, 2264−2275.
(48) Wu, W.; Zeng, Y.; Li, X.; Zhang, X.; Zheng, S.; Meng, L. Interplay between Halogen Bonds and Hydrogen Bonds in OH/SH···HOX···HY (X = Cl, Br; Y = F, Cl, Br) Complexes. *J. Mol. Model.* **2013**, *19*, 1069−1077.
(49) Pedzisa, L.; Hay, B. P. Aliphatic C-H···Anion Hydrogen Bonds: Weak Contacts or Strong Interactions? *J. Org. Chem.* **2009**, *74*, 2554−2560.
(50) Azofra, L. M.; Scheiner, S. Complexes Containing CO_2 and SO_2. Mixed Dimers, Trimers and Tetramers. *Phys. Chem. Chem. Phys.* **2014**, *16*, 5142−5149.
(51) Mohan, N.; Vijayalakshmi, K. P.; Koga, N.; Suresh, C. H. Comparison of Aromatic NH···π, OH···π, and CH···π Interactions of Alanine Using MP2, CCSD, and DFT Methods. *J. Comput. Chem.* **2010**, *31*, 2874−2882.
(52) Boys, S. F.; Bernardi, F. The Calculation of Small Molecular Interactions by the Differences of Separate Total Energies. Some Procedures with Reduced Errors. *Mol. Phys.* **1970**, *19*, 553−566.
(53) Reed, A. E.; Weinhold, F.; Curtiss, L. A.; Pochatko, D. J. Natural Bond Orbital Analysis of Molecular Interactions: Theoretical Studies of Binary Complexes of HF, H_2O, NH_3, N_2, O_2, F_2, CO and CO_2 with HF, H_2O, and NH_3. *J. Chem. Phys.* **1986**, *84*, 5687−5705.
(54) Reed, A. E.; Curtiss, L. A.; Weinhold, F. Intermolecular Interactions from a Natural Bond Orbital, Donor-Acceptor Viewpoint. *Chem. Rev.* **1988**, *88*, 899−926.
(55) Szalewicz, K.; Jeziorski, B. Symmetry-Adapted Perturbation Theory of Intermolecular Interactions. In *Molecular Interactions. From Van der Waals to Strongly Bound Complexes*; Scheiner, S., Ed.; Wiley: New York, 1997; pp 3−43.
(56) Moszynski, R.; Wormer, P. E. S.; Jeziorski, B.; van der Avoird, A. Symmetry-Adapted Perturbation Theory of Nonadditive Three-Body Interactions in van der Waals Molecules. I. General Theory. *J. Chem. Phys.* **1995**, *103*, 8058−8074.
(57) Werner, H.-J.; Knowles, P. J.; Manby, F. R.; Schütz, M.; Celani, P.; ; Knizia, G.; Korona, T.; Lindh, R.; Mitrushenkov, A.; Rauhut, G.; Adler, T. B.; et al. *Molpro*, version 2006; 2010. http://www.molpro.net/.
(58) Hopkins, W. S.; Hasan, M.; Burt, M.; Marta, R. A.; Fillion, E.; McMahon, T. B. Persistent Intramolecular C−H···X (X = O or S) Hydrogen-Bonding in Benzyl Meldrum's Acid Derivatives. *J. Phys. Chem. A* **2014**, *118*, 3795−3803.
(59) Gao, X.; Liu, Y.; Li, H.; Bian, J.; Zhao, Y.; Cao, Y.; Mao, Y.; Li, X.; Xu, Y.; Ozaki, Y.; Wu, J. A Cooperative Hydrogen Bonding System with a C-H···O Hydrogen Bond in Ofloxacin. *J. Mol. Struct.* **2013**, *1040*, 122−128.
(60) Scheiner, S.; Gu, Y.; Kar, T. Evaluation of the H-Bonding Properties of CH···O Interactions Based Upon NMR Spectra. *J. Mol. Struct.: THEOCHEM* **2000**, *500*, 441−452.
(61) Uldry, A.-C.; Griffin, J. M.; Yates, J. R.; Perez-Torralba, M.; Maria, M. D. S.; Webber, A. L.; Beaumont, M. L. L.; Samoson, A.; Claramunt, R. M.; Pickard, C. J.; et al. Quantifying Weak Hydrogen Bonding in Uracil and 4-Cyano-4′-Ethynylbiphenyl: A Combined Computational and Experimental Investigation of NMR Chemical Shifts in the Solid State. *J. Am. Chem. Soc.* **2008**, *130*, 945−954.
(62) Scheiner, S.; Kar, T.; Gu, Y. Strength of the $C^{\alpha}H$·O Hydrogen Bond of Amino Acid Residues. *J. Biol. Chem.* **2001**, *276*, 9832−9837.
(63) Yates, J. R.; Pham, T. N.; Pickard, C. J.; Mauri, F.; Amado, A. M.; Gil, A. M.; Brown, S. P. An Investigation of Weak CH···O Hydrogen Bonds in Maltose Anomers by a Combination of Calculation and Experimental Solid-State NMR Spectroscopy. *J. Am. Chem. Soc.* **2005**, *127*, 10216−10220.
(64) Scheiner, S.; Kar, T.; Pattanayak, J. Comparison of Various Types of Hydrogen Bonds Involving Aromatic Amino Acids. *J. Am. Chem. Soc.* **2002**, *124*, 13257−13264.
(65) Bent, H. A. Electronegativities from Comparison of Bond Lengths in AH and AH^+. *J. Chem. Phys.* **1960**, *33*, 1258−1259.
(66) Alabugin, I. V.; Manoharan, M.; Peabody, S.; Weinhold, F. Electronic Basis of Improper Hydrogen Bonding: A Subtle Balance of Hyperconjugation and Rehybridization. *J. Am. Chem. Soc.* **2003**, *125*, 5973−5987.
(67) Li, A. Y. Chemical Origin of Blue- and Redshifted Hydrogen Bonds: Intramolecular Hyperconjugation and Its Coupling with Intermolecular Hyperconjugation. *J. Chem. Phys.* **2007**, *126*, 154102.
(68) Pluháková, K.; Hobza, P. On the Nature of the Surprisingly Small (Red) Shift in the Halothane···Acetone Complex. *ChemPhysChem* **2007**, *8*, 1352−1356.
(69) Grabowski, S. J. Red- and Blue-Shifted Hydrogen Bonds: The Bent Rule from Quantum Theory of Atoms in Molecules Perspective. *J. Phys. Chem. A* **2011**, *115*, 12789−12799.
(70) Deakyne, C. A.; Meot-Ner, M. Unconventional Ionic Hydrogen Bonds. 2. NH^{+}···π. Complexes of Onium Ions with Olefins and Benzene Derivatives. *J. Am. Chem. Soc.* **1985**, *107*, 474−479.
(71) Meot-Ner, M.; Deakyne, C. A. Unconventional Ionic Hydrogen Bonds. 1. $CH^{\delta+}$···X. Complexes of Quaternary Ions with n- and π-Donors. *J. Am. Chem. Soc.* **1985**, *107*, 469−474.
(72) Kim, K. S.; Lee, J. Y.; Lee, S. J.; Ha, T.-K.; Kim, D. H. On Binding Forces between Aromatic Ring and Quaternary Ammonium Compound. *J. Am. Chem. Soc.* **1994**, *116*, 7399−7400.
(73) Lee, J. Y.; Lee, S. J.; Cho, H. S.; Cho, S. J.; Kim, K. S.; Ha, T.-K. Ab Initio Study of the Complexation of Benzene with Ammonium Cations. *Chem. Phys. Lett.* **1995**, *232*, 67−71.
(74) Liu, T.; Gu, J.; Tan, X.-J.; Zhu, W.-L.; Luo, X.-M.; Jiang, H.-L.; Ji, R.-Y.; Chen, K.-X.; Silman, I.; Sussman, J. L. Theoretical Insight into the Interactions of TMA-Benzene and TMA-Pyrrole with B3LYP Density-Functional Theory (DFT) and Ab Initio Second Order Møller-Plessest Perturbation Theory (MP2) Calculations. *J. Phys. Chem. A* **2001**, *105*, 5431−5437.

(75) Pullman, A.; Berthier, G.; Savinelli, R. Theoretical Study of Binding of Tetramethylammonium Ion with Aromatics. *J. Comput. Chem.* **1997**, *18*, 2012−2022.
(76) Liu, T.; Gu, J.; Tan, X.-J.; Zhu, W.-L.; Luo, X.-M.; Jiang, H.-L.; Ji, R.-Y.; Chen, K.-X.; Silman, I.; Sussman, J. L. The Relationship between Binding Models of TMA with Furan and Imidazole and the Molecular Electrostatic Potentials: DFT and MP2 Computational Studies. *J. Phys. Chem. A* **2002**, *106*, 157−164.
(77) Ansorg, K.; Tafipolsky, M.; Engels, B. Cation-π Interactions: Accurate Intermolecular Potential from Symmetry-Adapted Perturbation Theory. *J. Phys. Chem. B* **2013**, *117*, 10093−10102.
(78) Tsuzuki, S.; Honda, K.; Uchimaru, T.; Mikami, M.; Tanabe, K. The Interaction of Benzene with Chloro- and Fluoromethanes: Effects of Halogenation on CH/π Interaction. *J. Phys. Chem. A* **2002**, *106*, 4423−4428.
(79) Fujii, A.; Shibasaki, K.; Kazama, T.; Itaya, R.; Mikami, N.; Tsuzuki, S. Experimental and Theoretical Determination of the Accurate Interaction Energies in Benzene−Halomethane: The Unique Nature of the Activated CH/π Interaction of Haloalkanes. *Phys. Chem. Chem. Phys.* **2008**, *10*, 2836−2843.
(80) López, J. C.; Caminati, W.; Alonso, J. L. The CH$\cdots\pi$ Hydrogen Bond in the Benzene-Trifluoromethane Adduct: A Rotational Study. *Angew. Chem., Int. Ed. Engl.* **2006**, *45*, 290−293.
(81) Duarte, D. J. R.; de las Vallejos, M. M.; Peruchena, N. M. Topological Analysis of Aromatic Halogen/Hydrogen Bonds by Electron Charge Density and Electrostatic Potentials. *J. Mol. Model.* **2010**, *16*, 737−748.